J Solid State Electrochem (2016) 20:2427–2433
DOI 10.1007/s10008-016-3182-y

ORIGINAL PAPER

Detection of hydrogen peroxide releasing from prostate cancer cell using a biosensor

Bruno P. Crulhas[1] · **Naira P. Ramos**[1] · **Gustavo R Castro**[1] · **Valber A. Pedrosa**[1]

Received: 28 October 2015 / Revised: 7 March 2016 / Accepted: 13 March 2016 / Published online: 23 March 2016

Abstract In this work, highly sensitive and selective hydrogel microstructures to detect hydrogen peroxide releasing from cancer cell based on electrochemical biosensors are proposed. Gold nanoparticles (AuNPs) were conjugated with horseradish peroxidase and were dispersed in the prepolymer solution of poly(ethylene glycol) diacrylate. The prepolymer solution was photolithographically patterned in alignment with an array of Au microelectrodes fabricated on glass. Performance of this biosensor was characterized by transmission electron microscopy, electrochemical impedance spectroscopy, and cyclic voltammetry. Under the optimal condition, the proposed biosensor can detect hydrogen peroxide (H_2O_2) in a wide linear range from 2 to 100 μM with a low detection limit of 0.01 μM. It can be also directly used to mark out extracellular H_2O_2 released from prostate cells. Furthermore, the reproducibility, stability, and selectivity of the biosensor are analogous with the previous report, so this methodology can be used in physiological and pathological detection of H_2O_2 in the future.

Introduction

Overall, inflammation is now recognized as a central feature of prevalent pathologies, such as atherosclerosis, inflammatory bowel disease, autoimmune disease, and cancer [1, 2]. Several research groups have focused on regulation of an inflammatory response to better understand reactive oxygen species (ROS) that arise through oxidative process. Hydrogen peroxide has been studied as ROS with a long known function during progressive inflammation step. As a by-product of oxidative metabolism in vivo, H_2O_2 is also known as the most stable reactive oxygen species implicated in cell proliferation, aging, death, and signal transduction [3, 4]. Also, it is involved in many regulatory cellular events including the activation of transcription factors, cell proliferation, and apoptosis [5]. In addition, H_2O_2 produced from the mitochondrial electron transport chain has been shown to play a role in hematopoietic cell differentiation and cell division in flies [6], and is capable of modulating a number of principal signaling cascades including ERK, JNK, p38, MAPK, and PI3K/Akt [7, 8]. As a result, H_2O_2 is an important indicator of inflammation and may serve as a diagnostic marker of the immune system.

Over the past decades, numerous researchers have worked on the development of integration of biological and sensing components that can be used in vitro [9–11]. Much effort is devoted to the immobilization of the different enzymes using different materials that can enhance sensor sensitivity and specificity [12, 13]. Recently, electrodes modified with nanostructure have exhibited excellent enhancement of electrons-transfer effects leading to unique optical, electronic, and catalytic properties [14, 15]. The dimensions of these particles make them ideal candidates for the fabrication of functional nanostructures. Particularly, the combination of nanoparticle metals with hydrogel matrixes have attracted substantial research efforts directed to the development of the sensing materials that make them potential candidate materials to play the catalytic role in fabrication of a biosensing system [16, 17]. Gold nanoparticle is one of the most studied nanomaterial that has excellent conductivity and catalytic properties, which makes it suitable for acting as “electronic wires” to enhance the electron transfer between redox centers in proteins and electrode surfaces, and as catalyst to increase electrochemical

✉ Valber A. Pedrosa
vpedrosa@ibb.unesp.br

[1] Universidade Estadual Paulista Julio de Mesquita Filho, Botucatu, SP, Brazil

reactions. Due to its large specific surface area and high surface free energy, gold nanoparticles can adsorb biomolecules strongly and play an important role in the immobilization of biomolecules in biosensor construction. Also, it has been shown that the properties of nanostructures can be enhanced by the conductive environment provided by the polymeric matrixes. In particular, the incorporation of gold nanoparticle in conductive polymers is of interest because of the strong electronic interactions between the nanoparticle and the polymeric matrixes [18]. Recently, different authors have published alternative ways to adjust properties of hydrogels with nanoparticles, permitting the tuning or creation of new properties of the composite relative to the individual components [19, 20]. In all of these previous methods, the biological components are deposited onto the polymer which can decrease the electron transfer rate constants. This decrease can be attributed to the lack of alignment of bioelectrocatalyst with the electrode surface.

In this study, an easy method to detect hydrogen peroxide release from cancer cell using a micropatterned biosensor is constructed. The combined polymer/nanoparticle does not only strikingly improve the sensitivity of different substrate, but also provides good repeatability and reproducibility, thus, can be potentially exploited for future studies in vitro to monitor cell metabolite fluxes.

Experimental section

Materials

Poly(ethylene)glycol diacrylate (PEG-DA, MW 575), 2-hydroxy-2-methyl-propiophenone (photoinitiator), 99.9 % toluene, horseradish peroxidase (HRP) (EC 1.11.1.7, type VI-A), mercapto-carboxylic acid (MUA), ferrocene monocarboxylic acid (FcMA), hydrogen peroxide, N-hydroxysuccinimide (NHS), 1-ethyl-3-(3-dimethylaminopropyl) carbodiimide (EDC), 3-(trichlorosilyl) propyl methacrylate, gold(III)chloride, and sodium citrate dihydrate were purchased from Sigma (St Louis, MO). Phosphate buffer (PBS) 0.1 M was used as an electrolyte for all electrochemistry experiments. Water used for preparation of aqueous solutions came from a Millipore Direct-Q water purification system (resistivity, 18 MΩ cm^{-2}). Stock solutions were prepared in Milli-Q water and stored at 4 °C.

Preparation of prostate cancer cells

PC-3 human prostate cancer cell lines (ATCC® CRL-1435™) is a well-known lineage type used in prostate cancer research. These cells are useful in investigating biochemical changes in advanced prostatic cancer cells. Cells were cultivated in 75 cm^2 flask in Roswell Park Memorial Institute Media supplemented with fetal bovine serum, L-glutamine and streptomycin (10 mg), and penicillin (10,000 U). All reagents were purchased from Gibco® (Waltham, MA). Cells were cultivated until they reached at least 90 % of confluency. Right after, cells were trypsinized by using trypsin-EDTA (Gibco®, Waltham, MA). Cells viability was evaluated by Neubauer chamber method.

Design of Au electrode arrays

Electrode layout was made in AutoCAD and transformed into plastic transparencies by DGM design (Curitiba, Brazil). Fabrication of gold electrode arrays, were made at the Brazilian Nanotechnology National Laboratory (LNNano-CNPEM, Campinas/SP). Sputter-coated standard (75 mm × 25 mm) glass slides were developed with 15 nm Cr adhesion layer and 100 nm Au layer. Electrodes were produced by photoresist lithography and wet etching. Etching of Au/chrome layers in an array of eight working microelectrodes patterned on a glass slide. Each Au electrode was 300 μm in diameter with 15 μm wide leads and 1 mm × 1 mm square contact pad (Fig. 1a).

Establishment of gold nanoparticles HRP-carrying hydrogel microstructures on Au electrode arrays

Gold nanoparticles were synthesized by standard wet chemical methods using sodium citrate as a reducing agent, and MUA-AuNPs were conjugated by ligand exchange between

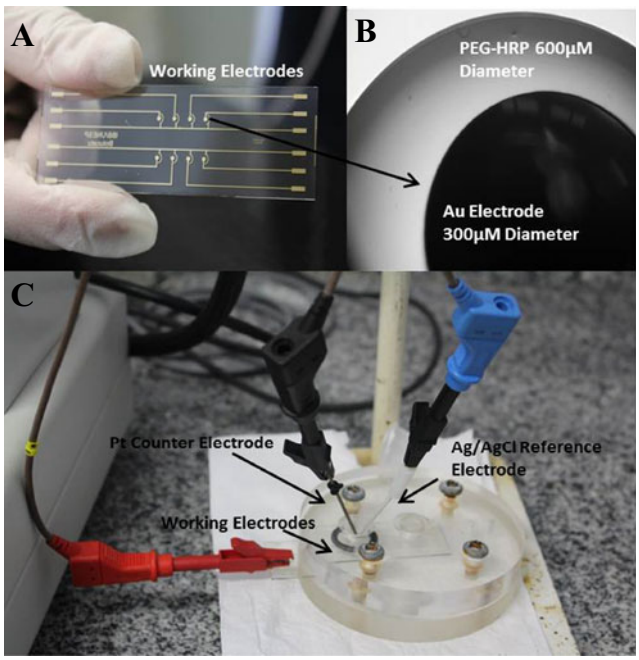

Fig. 1 **a** Overview of sensing chip containing eight micropatterned Au electrodes. **b** PEG-HRP polymerized on top of Au electrode. **c** Electrochemical experiments containing Ag/AgCl as reference, Pt wire as counter, and patterned Au as working electrodes

mercapto-carboxylic acid and citrate-stabilized gold nanoparticles (AuNPs), by previous reported papers [21]. The gold nanoparticle was analyzed by uv-vis spectrum. Briefly, 0.5 mL suspension of Au nanoparticle was gently added to 0.5 mL MUA solution (70 % of ethanol) and stirred for 4 h. Subsequently, the mixture was centrifuged at 9000 rpm for 15 min to remove excess alkanethiol and resuspended in phosphate buffer (10 mM, pH 6.5).

Attachment of enzyme horseradish peroxidase to MUA/AuNP was prepared using EDC/NHS conjugation. In summary, 1 mL MUA-AuNPs solution was incubated and stirred for 2 h with 100 mM NHS and 200 mM EDC solution and finally added 0.1 mL of HRP solution (15 mg/mL in 10 mM of PBS at pH 6.0) and left stirring overnight. Quality of AuNPs was verified by electro transfer microscopy (Fig. 2a, b).

Simultaneous with the HRP-AuNPs preparation, prepolymer solution containing PEG-DA and 2 % (*v*/*v*) photoinitiator (2-hydroxy-2-methyl-propiophenone) was made and mixed with 0.1 mL of HRP-AuNPs by sonication for 1 min and then stirred overnight at 4 °C. Prior to the immobilization of hydrogel, glass slides were silanized as following standard protocol. Briefly, glass slides were cleaned in "piranha" solution consisting of 3:1 ratio of H_2SO_4 and H_2O_2 for 30 min, washed in Milli-Q water, and subsequently immersed in 2 mM toluene solution of 3-(trichlorosilyl) propyl methacrylate (TPM) for 1 h to obtain a self-assembled silane monolayer then substrates were washed to remove excess of silane agent and placed in an oven for 3 h at 100 °C to crosslink the silane layer.

The PEG-based prepolymer solution was spin-coated at 800 rpm for 4 s onto glass slides containing Au electrode patterns. A photomask was registered with an electrode pattern and then exposed to UV light at 65 mW/cm^2 for 10s to convert liquid prepolymer into cross-linked hydrogel. Surfaces were developed in DI water for 3 min to remove the unpolymerized PEG precursor solution. Enzyme-AuNPs carrying hydrogel microstructures were made larger than Au electrodes; feature sizes were 600 and 300 mm in diameter for hydrogel elements and Au electrodes, respectively. This was done to ensure effective anchoring of the hydrogel structures to silanized glass substrates (Fig. 1b).

Electrochemical detection of H_2O_2

A potentiostat μAutoLabIII (Metrohn, NL) was employed for the cyclic voltammetry (CV) experiments. The electrochemical cell consisted of an Ag/AgCl (3 M KCl) reference electrode, a platinum wire counter electrode placed, and Au working electrodes positioned inside the electrochemical cell (Fig. 1c); all experiments were done in quintuplicates.

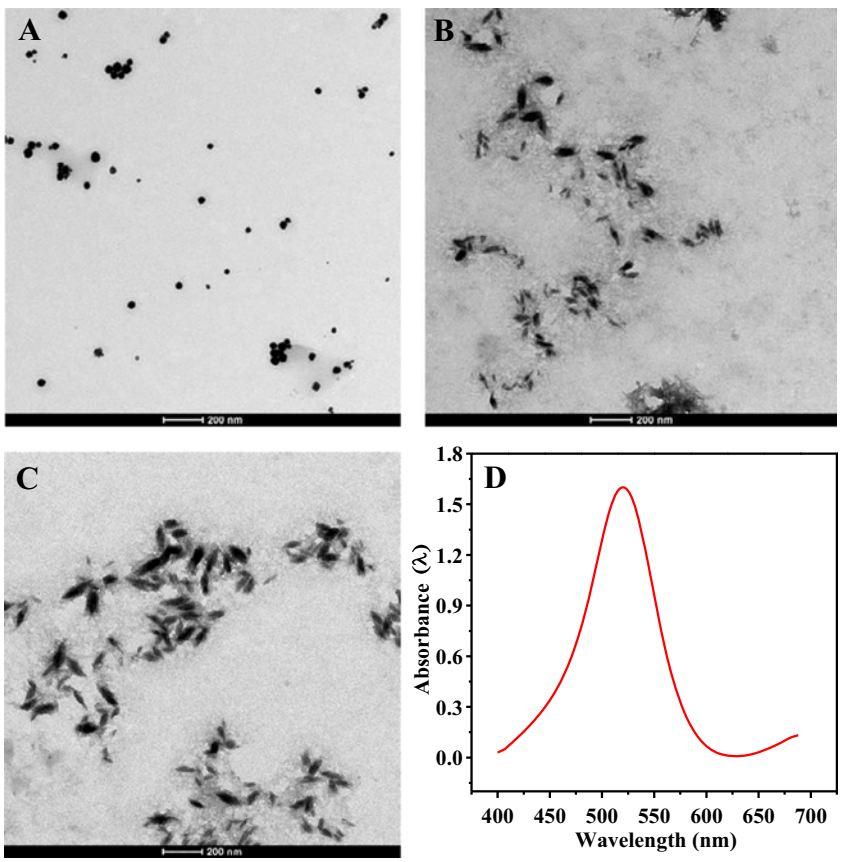

Fig. 2 **a** Transmission electron microscopy (TEM) images of gold nanoparticle. **b** TEM images of HRP conjugated with AuNP. **c** TEM images of HRP/AuNPs dispersed into PEG-hydrogel matrix. **d** The UV-vis spectrum of AuNPs

Cyclic voltammetry was used to detect H_2O_2 by PEG-HRP-AuNPs electrodes. Briefly, several H_2O_2 concentrations were prepared in PBS and infused into the electrochemical cell containing enzyme-AuNPs-based electrodes and analyzed by cyclic voltammograms from 0.8 to −0.8 V at the scan rate of 50 mV/s. For validating the specificity, the biosensor was tested in the presence of interfering compounds (10 mM of ascorbic acid and 10 mM of uric acid).

Calibration curve was constructed by plotting absolute value for reduction current at −0.4 V versus H_2O_2 concentration when compared to control without hydrogen peroxide. Limit of detection (LOD) was calculated based on calibration curve using linear regression by the standard deviation of y-intercept (LOD = 3σ/slope), and sensitivity was calculated using working electrode surface area.

To detect H_2O_2 production from prostate cancer cells (PC3), cells were incubated onto the surface of the electrode. PC3 cells are an aggressive type of prostate cancer, and association between prostatic cancer and oxidative stress has been well-recognized. There is considerable evidence suggesting oxidative stress contributes to the etiology and pathogenesis of the prostate cancer; therefore, small amount of hydrogen peroxide is naturally released by PC3 cells [22]. Briefly, prior to seeding of the cells, the surface was treated with 0.2 mg/mL of collagen (I) to promote cell attachment. Subsequently, PC3 cells were suspended in cell culture medium at a concentration of 106 cells mL^{-1} and incubated at 37 °C over the surface of the biochip for 1 h. CV measurements were made every 20 min during the 2.5 h.

Results and discussion

Electrochemical characterization of enzyme-AuNPs biosensors

HRP-AuNPs-PEG sensor was manufactured by polymerizing enzyme–hydrogel on top of micropatterned Au electrodes (Fig. 1b). HRP enzyme with AuNPs was conjugated and incorporated into hydrogel microstructures in order to increase sensitivity and stability of the biosensor and also optimize enzyme retention into hydrogel.

The morphology of modified AuNP was characterized by TEM. Figure 2 a shows the well-dispersed AuNP with a size of about 22 nm in diameter, and also by Uv-vis spectrum of AuNPs particles with a peak at 520 nm (Fig. 2d). The microstructural investigation of AuNPs-HRP was carried out using TEM to reveal size, shape, and distribution of the particles. From the micrographs, it is observed that an aggregation step and the size of particles increased due to the presence of the enzyme (Fig. 2b). The size of spherical thiolated gold nanoparticles conjugated with HRP is found to be varying around 30 to 50 nm. Figure 2c shows the dispersion of AuNPs into PEG matrix being similar to dispersion of AuNPs in buffer.

To characterize the voltammetric behavior of the biosensor, a set of experiments was conducted using cyclic voltammetry in the presence of 0.5 mM FcMA in 10 mM PBS buffer at scan rates varying from 20 to 250 mV s^{-1}. The results obtained show that with increased scan rate, the redox peak current also increased gradually (Fig. 3a). The correlation of redox peak currents with scan rate is shown in Fig. 3c. Peak currents were

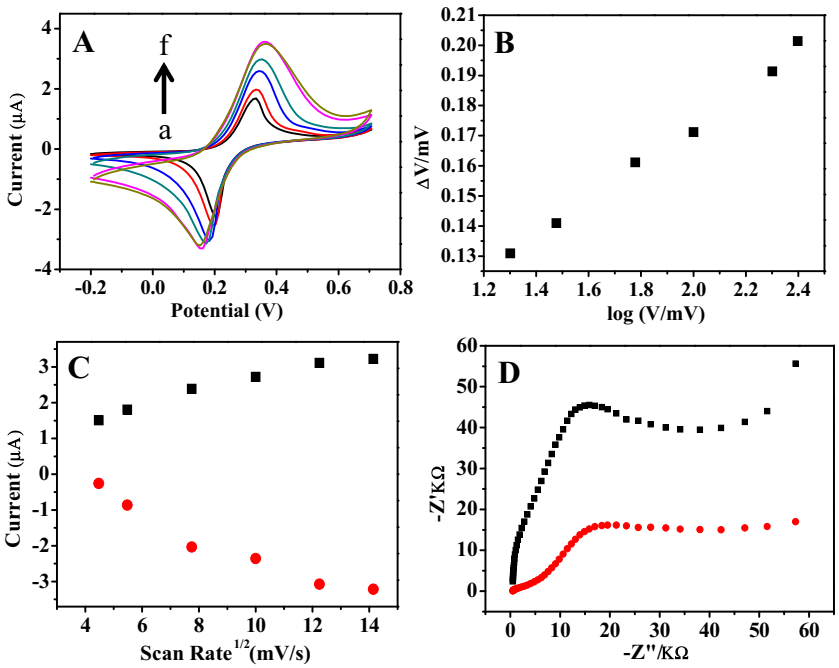

Fig. 3 **a** Cyclic voltammograms of HRP-AuNP-PEG Au electrode at different scan rates (*a–f* 20, 30, 60, 100, 200, and 250 mV/s) in the presence of 0.5 mM FcMA in 10 mM PBS buffer (pH 6.5). **b** Peak-to-peak separation as a function of the potential scan rate. **c** Plot of redox peaks current versus square root of scan rate, cathodic peak (*red circle*), and anodic peak (*black square*) HRP-AuNP-PEG. **d** Impedance spectroscopy PEG-Au electrodes. Nyquist plots for PEG/Au electrodes containing HRP-PEG (*black square*) and (*red circle*) HRP-AuNP-PEG frequency intervals were from 0.1 Hz to 1 mHz

proportional to square root of scan rate ($\upsilon^{1/2}$), which indicates a diffusion controlled process. To better understand, the reaction mechanism was analyzed by peak potential versus scan rate. Separation of peak-to-peak (ΔEp) remains nearly constant up to 60 mV, which suggests an electrochemical process reversibly confined surface (Fig. 3b).

In addition, electrochemical impedance spectroscopy (EIS) experiments were used to evaluate charge transfer resistance. Figure 3d displays typical Nyquist plots of impedance of various electrodes recorded in a frequency range of 0.1 Hz–100.0 kHz in PBS (0.05 M, pH 7.2) containing 0.5 mM FcMA in 10 mM of PBS. Electron-transfer kinetics such as charge transfer resistance (R_{ct}), solution resistance (R_s), double layer capacitance (C_d), and a mass transfer element W (Warburg impedance) could be extracted by EIS data fitting. The electron-transfer resistance (R_{et}, the diameter of semicircle) of redox probe measuring ferrocene reactivity on gold microelectrode (red line) and after enzyme attached (black line) were 30 and 45 KΩ, respectively (Fig. 3d). This means that the resistance increased with the enzyme deposited on top of the microelectrode. [23].

H_2O_2 is an electroactive compound, and it was a verified reduction process in absence and presence of HRP conjugated with AuNPs and PEG hydrogel. CVs of step by step preparation of electrode in the presence of H_2O_2 was done to ensure that the incorporation of redox enzyme conjugated with AuNPs in hydrogel matrix increased current response in both positive and negative potential ranges when compared to response for only hydrogel or AuNP-Hydrogel (Fig. 4a). Therefore, increase in reduction current was obtained by adding H_2O_2 into electrochemical cell containing microelectrodes, which indicates reduction and diffusion of H_2O_2 to hydrogel. In contrast, electrodes made with only pure PEG did not show changes in current when challenged with H_2O_2 (Fig. 4a).

Thus, it validates that HRP enhances with the reduction of H_2O_2. Calibration curve of enzyme-AuNPs sensor was performed by spiking known concentrations of H_2O_2 into the device containing HRP-AuNPs-PEG electrodes and used CV to monitoring reduction current in range of 0.8 to −0.8 V. Injected with different concentrations of H_2O_2 diffuses it into hydrogel matrix and reacts with HRP entrapped inside

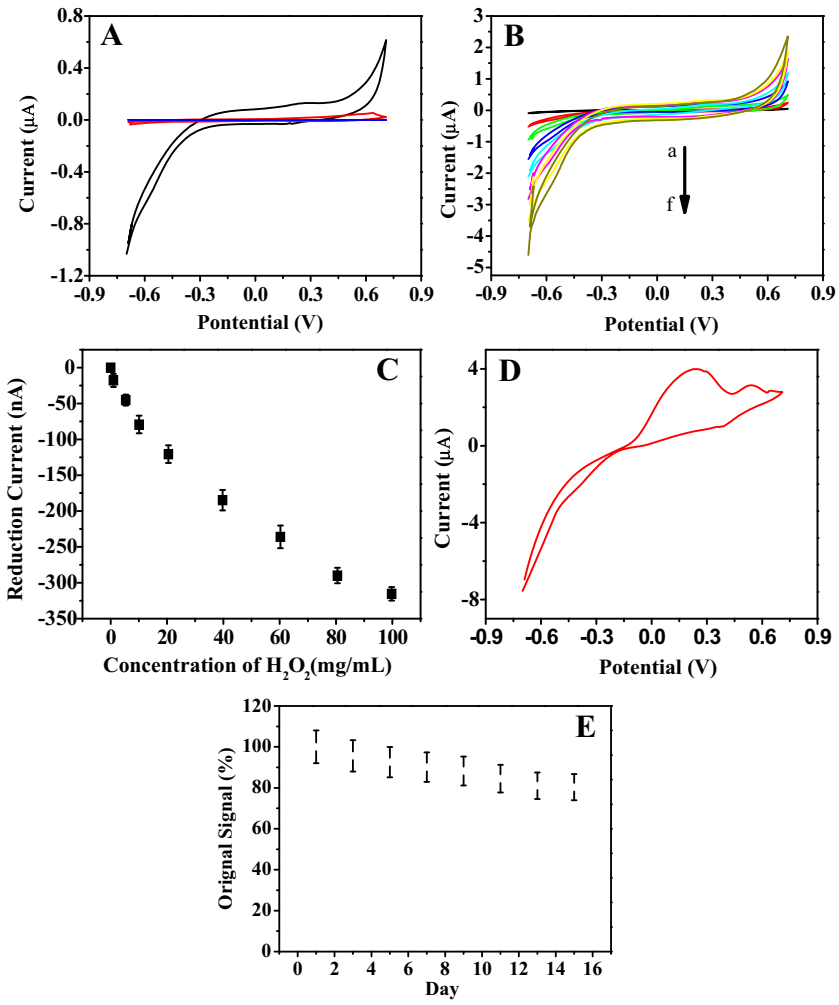

Fig. 4 **a** CV plots of PEG (*blue line*), AuNP-PEG(*red line*), and HRP-AuNP-PEG(*black line*) polymerized onto Au electrodes in the potential range of 0.7 to −0.7 V at the scan rate of 50 mV/s and in the presence of 5 mg/mL of H_2O_2. **b** CV plots of the PEG-HRP electrode as a function of H_2O_2 (*a–f* 1, 5, 10, 20, 50, and 100 mg/mL). The reductive current increases with increasing concentration of H_2O_2. This indicates enhanced enzymatic reaction between HRP and H_2O_2. **c** Calibration plot obtained for HRP-AuNP-PEG electrode showing absolute value of the reduction current as a function of different H_2O_2 concentrations. **d** CV plots of HRP-AuNP-PEG. **e** Reproducibility plot of HRP-AuNP-PEG biosensor

the hydrogel (Fig. 4b). Figure 4c shows calibration plot (reduction current versus H_2O_2 concentration at −0.4 V) for detection of H_2O_2. The low operating potential (−0.4 V) was used because it avoids interference due to other competitive species such as ascorbic acid and uric acid [24].

In order to avoid unspecific interaction with small molecules generally found in physiological fluids, like ascorbic acid and uric acid, we verified the effects of these interfering compounds into our biosensor by CVs and it was able to detect H_2O_2 in the presence of high concentrations of ascorbic acid and uric acid because reduction signal of H_2O_2 was evaluated at −0.4 V and the peak of ascorbic acid and uric acid appeared at 0.2 and 0.6 V, respectively Fig. 4d.

The lowest concentration of H_2O_2 that could be detected by each sensing electrode of area 0.0708 mm^2 was found to be 0.01 μM (R^2 = 0991). Sensitivity of the sensor was calculated to be 18.5 nA μM/mm^2. Stability of enzyme − AuNPs-hydrogel electrode was verified at a regular interval of 1 week by infusing a 20-μM concentration of H_2O_2 in the electrochemical cell with HRP-AuNPs-PEG sensor.

The HRP-PEG-AuNPs biosensors were highly reproducible with a standard deviation of 8 % in hydrogen peroxide detection. The working electrode was stable after 2 weeks of testing. Coupling of AuNPs with PEG hydrogels provides an excellent matrix for electrochemical detection due to inclusion of redox sites into the hydrogel being a reliable tool for use in clinical diagnostics.

Electrochemical detection of H_2O_2 released by prostate cancer cells

To conduct biological experiments with prostate cancer, PC3 cells were seeded onto collagen (I)-coated surfaces containing enzyme-AuNPs electrodes (Fig. 5a, b). The device containing cells and electrode were kept in a tissue culture incubator at 37 °C for 24 h. Prostate cancer cells did not attach on top of electrodes due to non-fouling properties of PEG. An estimated 1,000,000,00 cells were cultured inside the electrochemical cell during sensing experiment.

Release of H_2O_2 was detected with CV by diffusion of H_2O_2 inside hydrogel, and measurements were made every 20 min in a span of 2.5 h. Increase in reduction current of H_2O_2 was observed right after first measurement, showing constant production of H_2O_2 from PC3 cells (Fig. 5c). Reduction current did not saturate after 2.5 h, proving the feasibility and stability of the sensor which was not compromised by non-specific proteins and by-product released by PC3 cells. Figure 5c represents reduction current response to PC3 cells to H_2O_2. Further, a control experiment was done using the same methodology of modified hydrogel patterned on electrodes without HRP and was designed to test whether detection of cellular response requires the presence of peroxide-specific enzyme HRP. In the absence of HRP, no reductive current was detected. This control experiment further validated that the analyte produced by cells and detected at the sensing electrodes was indeed H_2O_2.

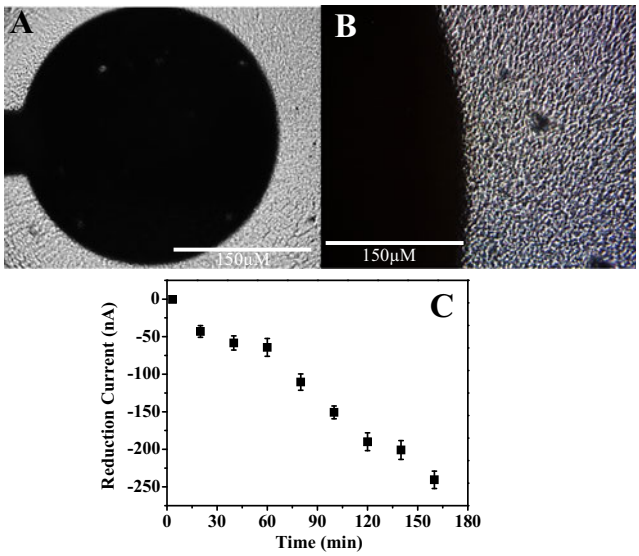

Fig. 5 Sensor surface. **a** Microscopy image 10× of PC3 cells seeding onto collagen-modified silane region around HRP-AuNP-PEG electrode. **b** Microscopy image 40× of PC3 cells seeding onto collagen-modified silane region around HRP-AuNP-PEG electrode. **c** Plot showing absolute value of the reduction current as a function of H_2O_2 released by cells

The biosensor is the first one to use enzymes coupled with AuNPs and hydrogel to detect H_2O_2 released by cancer cells; the majority of this type of platform is used to detect ROS released by immune cells [24–27]. Similar experiments were made by Revzin et al. [28] and when compared with similar sensors found in literature, the sensor used in this work achieved better results from sensitivity, stability, and limit of detection (Table 1).

Conclusion

The study describes the use of enzyme-AuNPs-PEG electrodes to enable detection of H_2O_2 from cancer cells by a photolithography process. The biosensor had a detection limit of 0.01 μM H_2O_2 with linear range extending to 100 μM. A microsystem utilizing enzyme-AuNPs-based electrodes was

Table 1 Comparison of analytical performance of H_2O_2 biosensor

H_2O_2 biosensor	Detection limit (mM)	Reference
HRP-AuNP-PEG	0.001	This work
HRP-AuNP	0.003	[29]
HRP-ferrocene	2.32	[30]
HAP-α-zirconium phosphate/GC	12	[31]
HRP-nano-Au-carbon ceramic	61	[32]
HRP-DNA/GC	25	[33]

used to detect prostate cancer cell production of H_2O_2 that ranged from 0.07 μM at 20 min to 2.36 μM after 2.5 h. Due to conjugation of enzyme with AuNPs inside the hydrogel, the biosensor achieved excellent stability and feasibility due to PEG non-fouling properties. Moreover, it can be also used to efficiently monitor the extracellular H_2O_2 released from human prostate cancer cells. Therefore, this biosensor might be useful for the further physiological and pathological applications, like cancer and inflammatory process that releases hydrogen peroxide.

Acknowledgments We gratefully acknowledge partial support by grants from the FAPESP (2014/05653-5, 2012/15666-1), CNPq, and CAPES.

References

1. Coussens LM, Werb Z (2002) Inflammation and cancer. Nature 420:860–867
2. Serhan CN, Savill J (2005) Resolution of inflammation: the beginning programs the end. Nat Immunol 6:1191–1197
3. Henzler T, Steudle E (2000) Transport and metabolic degradation of hydrogen peroxide in *Chara corallina*: model calculations and measurements with the pressure probe suggest transport of H_2O_2 across water channels. J Exp Bot 51:2053–2066
4. Lindahl T (1993) Instability and decay of the primary structure of DNA. Nature 362:709–715
5. Rojkind M, Domínguez-Rosales JA, Nieto N, Greenwel G (2002) Role of hydrogen peroxide and oxidative stress in healing responses. Cell Mol Life Sci 59:1872–1891
6. Bedard K, Krause KH (2007) The NOX family of ROS-generating NADPH oxidases: physiology and pathophysiology. Physiol Rev 87:245–313
7. Hensley K, Robinson KA, Gabbita SP, Salsman S, Floyd RA (2000) Reactive oxygen species, cell signaling, and cell injury. Free Radic Biol Med 28:1456–1462
8. Gabbita SP, Robinson KA, Stewart CA, Floyd RA, Hensley K (2000) Redox regulatory mechanisms of cellular signal transduction. Arch Biochem Biophys 376:1–13
9. Liu Y, Kwa T, Revzin A (2012) Simultaneous detection of cell-secreted TNF-a and IFN-g using micropatterned aptamer-modified electrodes. Biomaterials 33(30):7347–7355
10. Yan J, Pedrosa VA, Simonian AL, Revzin A (2010) Immobilizing enzymes onto electrode arrays by hydrogel photolithography to fabricate multi-analyte electrochemical biosensors. ACS Appl Mater Interfaces 2:748–755
11. Yan J, Pedrosa VA, Enomoto J, Simonian A, Revzin A (2011) Electrochemical biosensors for on-chip detection of oxidative stress. Biomicrofluidics 5(3):32008–32011
12. Pita M, Kramer M, Zhou J, Poghossian A, Schoning MJ, Fernandez VM, Katz E (2008) Optoelectronic properties of nanostructured ensembles controlled by biomolecular logic systems. ACS Nano 2:2160–2166
13. Tuleuova N, Jones CN, Yan J, Ramanculov E, Yokobayashi Y, Revzin A (2010) Development of an aptamer beacon for detection of interferon-gamma. Anaytical Chemistry 82:1851–1857
14. Pedrosa VA, Paliwal S, Balasubramanian S, Nepal D, Davis V, Wild J, Ramanculov E, Simonian A (2010) Enhanced stability of enzyme organophosphate hydrolase interfaced on the carbon nanotubes. Colloids and Surfaces B 77:69–74
15. Nemzer LR, Schwartz A, Epstein AJ (2010) Enzyme entrapment in reprecipitated polyaniline nano- and microparticles. Macromolecules 43:4324–4330
16. Jagur-Grodzinski J (2010) Polymeric gels and hydrogels for biomedical and pharmaceutical applications. Polymers for Advance Technol 21:27–47
17. Cong H, Revzin A, Pan T (2009) Non-adhesive PEG hydrogel nanostructures for self-assembly of highly ordered colloids. Nanotechnology 20(7):75307
18. Li J, Seok S, Chu B, Dogan F, Zhang Q, Wang Q (2009) Nanocomposites of ferroelectric polymers with TiO_2 nanoparticles exhibiting significantly enhanced electrical energy density. Adv Mater 21:217–221
19. Zhai D, Liu B, Shi Y, Pan L, Wang Y, Li W, Zhang R, Yu G (2013) Highly sensitive glucose sensor based on Pt nanoparticle/polyaniline hydrogel heterostructures. ACS Nano 7(4):3540–3546
20. Zhang R, Xu S, Luo J, Liu X (2015) Molecularly imprinted photosensitive polyglutamic acid nanoparticles for electrochemical sensing of hemoglobin. Microchim Acta 182:175–183
21. Pedrosa VA, Yan J, Simonian AL, Revzin A (2011) Micropatterned nanocomposite hydrogels for biosensing applications. Electroanalysis 23:1142–1149
22. Kumar B, Koul S, Khandrika L, Randall B, RB M, HK K (2008) Oxidative stress is inherent in prostate cancer cells and is required for aggressive phenotype. Cancer Res 68(6):1777–1785
23. Katz E, Willner I (2003) Probing biomolecular interactions at conductive and semiconductive surfaces by impedance spectroscopy: routes to impedimetric immunosensors, DNA-sensors, and enzyme biosensors. Electroanalysis 15(11):913–947
24. Heller I, Smaal WT, Lemay SG, Dekker C (2009) Probing macrophage activity with carbon-nanotube sensors. Small 22:2528–2532
25. Amatore C, Arbault S, Chen Y, Crozatier C, Tapsoba I (2007) Electrochemical detection in a microfluidic device of oxidative stress generated by macrophage cells. Lab Chip 7:233–238
26. Cheah LT, Dou YH, Seymour AML, Dyer CE, Haswell SJ, Wadhawanc JD, Greenman J (2010) Microfluidic perfusion system for maintaining viable heart tissue with real-time electrochemical monitoring of reactive oxygen species. Lab Chip 10:2720–2726
27. Li C, Zhang H, Wu P, Gong Z, Xu G, Cai C (2011) Electrochemical detection of extracellular hydrogen peroxide released from RAW 264.7 murine macrophage cells based on horseradish peroxidase–hydroxyapatite nanohybrids. Analust 136:1116–1123
28. Matharu Z, Enomoto J, Revzin A (2013) Electrochemical detection of hydrogen peroxide release from alcohol-injured hepatocytes with miniature enzyme-based electrodes. Anal Chem 85:932–939
29. Attar A, Cubillana-Aguilera L, Naranjo-Rodriguez I, Hidalgo de Cisneros JLH, Santander JMP, Amine A (2015) Amperometric inhibition biosensors based on horseradish peroxidase and gold sononanoparticles immobilized onto different electrodes for cyanide measurements. Bioelectrochemistry 101:84–91
30. Chinnadayyala SR, Kakoti A, Santhosh M, Goswami P (2014) A novel amperometric alcohol biosensor developed in a 3rd generation bioelectrode platform using peroxidase coupled ferrocene activated alcohol oxidase as biorecognition system. Biosensor and Bioelectronics 55:120–126
31. Yang X, Chen X, Yang L, Yang W (2008) Direct electrochemistry and electrocatalysis of horseradish peroxidase in α-zirconium phosphate nanosheet film. Bioelectrochemistry 74:90–95
32. Lei CX, Hu SQ, Gao N, Shen GL, Yu RQ (2004) An amperometric hydrogen peroxide biosensor based on immobilizing horseradish peroxidase to a nano-Au monolayer supported by sol–gel derived carbon ceramic electrode. Bioelectrochemistry 65:33–39
33. Zeng X, Li X, Liu X, Liu Y, Luo S, Kong B, Yang S, Wei W (2009) A third-generation hydrogen peroxide biosensor based on horseradish peroxidase immobilized on DNA functionalized carbon nanotubes. Biosens Bioelectron 25:806–900